Pyrazole Binding in Crystalline Binary and Ternary Complexes with Liver Alcohol Dehydrogenase†

Hans Eklund,* Jean-Pierre Samama,‡ and Leif Wallén

ABSTRACT: Pyrazole is a strong inhibitor of liver alcohol dehydrogenase in combination with oxidized coenzyme NAD^+. We have studied three different complexes of the inhibitor with the enzyme by using crystallographic methods: (1) the binary complex with pyrazole to 3.2-Å resolution, (2) the ternary complex with NAD^+–pyrazole to 2.9-Å resolution, and (3) the ternary complex with NAD^+–4-iodopyrazole to 2.9-Å resolution. Crystals of the binary complex are isomorphous to the apoenzyme, and pyrazole binds to the active-site zinc atom in a way analogous to imidazole. Crystals of the two ternary complexes are isomorphous with the ternary alcohol dehydrogenase–NADH–dimethyl sulfoxide complex. One of the nitrogen atoms of the pyrazole ring is directly bound to the active-site zinc atom with a Zn–N bond distance of 2.1 Å. The other nitrogen atom is 2 Å from the C4 atom of the nicotinamide ring of the coenzyme. The iodine atom in 4-iodopyrazole is located in the hydrophobic substrate cleft. The effect of substitutions on the pyrazole ring are discussed in relation to the structure of the active site and substrate pocket. Pyrazole derivatives with long alkyl chains bound in the 4 position are outstanding inhibitors, and this property is related to the topography of the hydrophobic substrate cleft. The conformation of the oxidized coenzyme in the ternary complexes is essentially the same as that of the reduced coenzyme NADH in the NADH–dimethyl sulfoxide complex.

Pyrazole and its derivatives have been extensively studied as inhibitors for liver alcohol dehydrogenase. They have been used in steady-state and fast kinetic experiments (Yonetani, 1963; Brand et al., 1967; Shore & Gilleland, 1970; Theorell & Tatemoto, 1971; McFarland & Bernhard, 1972; Jacobs et al., 1974; Reynolds & McKinley-McKee, 1975; Luisi et al., 1975; McFarland et al., 1977; De Traglia et al., 1977; Andersson, P., et al., 1981), in purification of the enzyme (Andersson et al., 1974; Lange & Vallee, 1976), and in experiments with enzyme where the active-site metal has been exchanged (Maret et al., 1980; Makinen & Yim, 1981), as well as for NMR (Bobsein & Meyers, 1981; Andersson, I., et al., 1981) and metabolic studies (Lester et al., 1968; Blomstrand & Theorell, 1970; Rydberg et al., 1972; Deis & Lester, 1979; Lieber, 1977). Some derivatives of pyrazole are the strongest inhibitors so far found for the enzyme (Tolf, 1981).

Theorell and co-workers found in their extensive investigation of the inhibitory power of imidazole and related compounds that the five-membered pyrazole ring was a strong inhibitor for the oxidation of alcohols. It forms a ternary complex with oxidized coenzyme NAD^+ and the enzyme (Theorell & Yonetani, 1963). In this complex NAD^+ was found to bind more tightly than if no pyrazole was present. The catalytic oxidation of ethanol is inhibited by imidazole with an inhibitor constant, K_I, of 7.6 mM, while pyrazole inhibits the ethanol oxidation several orders of magnitude more strongly, K_I = 0.2 μM (Theorell et al., 1969). Furthermore, derivatives of pyrazole with hydrophobic substitution in the 4 position were shown to be especially potent inhibitors (Theorell et al., 1969; Reynier, 1969; Dahlbom et al., 1974; Tolf et al., 1979; Tolf, 1981). 4-Iodopyrazole was found to have a K_I of 0.02 μM, 4-methylpyrazole, 0.08 μM, and 4-pentylpyrazole, 8×10^{-10} M. Substitution in the 3 and/or 5 position on the other hand decreases the inhibitory power.

Physiological and biochemical investigations on animals have shown that liver alcohol dehydrogenase has a fundamental role for endogenous and exogenous alcohol metabolism. In view of the large medical problem related to alcohol consumption as well as to methanol and ethylene glycol poisoning (Li, 1977), considerable interest has been focused on liver alcohol dehydrogenase inhibition. Recently a new form of human liver alcohol dehydrogenase has been discovered (Li et al., 1977; Bosron et al., 1979). This isozyme does not exhibit the same sensitivity toward pyrazole inhibition as the EE isozyme of horse liver alcohol dehydrogenase. The inhibitor constant by 4-methylpyrazole is 500 μM (Li et al., 1977) compared to 0.08 μM for the horse enzyme.

The ternary complex of alcohol dehydrogenase with pyrazole and oxidized coenzyme was one of the first ternary complexes to be crystallized (Theorell & Yonetani, 1963). Preliminary investigations of these crystals with X-ray diffraction were reported earlier (Brändén et al., 1965; Brändén, 1965; Zeppezauer et al., 1967), and 4-iodopyrazole was used as a heavy atom derivative (Eklund et al., 1981).

In this paper we report the crystallographic investigation of a binary complex of alcohol dehydrogenase with pyrazole isomorphous to the apoenzyme (Eklund et al., 1976) and to the binary complex with imidazole (Boiwe & Brändén, 1977), to which it is compared. We also report the crystallographic investigation of the ternary complexes of alcohol dehydrogenase and oxidized coenzyme with pyrazole and 4-iodopyrazole to 2.9-Å resolution. These complexes crystallize with triclinic symmetry isomorphous to the NADH–Me_2SO[1] complex (Eklund et al., 1981). We also report a model building study of probable binding modes for pyrazole derivatives by use of an interactive display system.

† From the Department of Chemistry and Molecular Biology, Swedish University of Agricultural Sciences, S-750 07 Uppsala 7, Sweden. *Received March 17, 1982.* This work was supported by grants from the Swedish Natural Science Research Council (Grant 2767) and from Centre National de la Recherche Scientifique to J.-P.S.

‡ Present address: Institut de Chimie, Université Louis Pasteur, F-76008 Strasbourg Cedex, France.

[1] Abbreviations: F_{obsd}, observed structure factors; F_{nat}, native structure factors; F_{calcd}, calculated structure factors; F_{der}, structure factors of a derivative; LADH, horse liver alcohol dehydrogenase (EC 1.1.1.1); MPD, 2-methyl-2,4-pentanediol; Me_2SO, dimethyl sulfoxide.

0006-2960/82/0421-4858$01.25/0

Table I: Crystallization Conditions of Complexes with LADH

inhibitor	concn (mM)	buffer	resolution (Å)	no. of crystals	no. of reflections
		Binary Complexes[a]			
imidazole[b]	5	5 mM imidazole/HCl, pH 7.8	2.9	8	8573
pyrazole	1	50 mM Tris-HCl, pH 8.4	3.2	3	6533
		Ternary Complexes[c]			
NAD^+	10				
pyrazole	1	50 mM Tes/NH_3, pH 7.0	2.9	2	16344
4-iodopyrazole	1	50 mM Tes/NH_3, pH 7.0	2.9	18	16344

[a] Orthorhombic crystals; cell dimensions: $a = 56.0$ Å, $b = 75.2$ Å, and $c = 181.7$ Å. [b] Data from Boiwe & Brändén (1977). [c] Triclinic crystals: $a = 51.8$ Å, $b = 44.5$ Å, $c = 94.3$ Å, $\alpha = 102°$, $\beta = 104°$, and $\gamma = 72°$.

Materials and Methods

Crystallization. Orthorhombic apoenzyme crystals were soaked with pyrazole to form the binary enzyme–pyrazole complex. Crystals of ternary complexes were obtained by dialysis of an enzyme solution, contained in dialysis bags, against increasing concentrations of 2-methyl-2,4-pentanediol (MPD) as described earlier (Eklund et al., 1981). Inhibitors and coenzyme were added to the outer solution at the beginning of the experiment. Crystallization conditions and concentrations of reagents are described in Table I. The triclinic crystals of the ternary complexes of enzyme with NAD^+–pyrazole and NAD^+–4-iodopyrazole were isomorphous to crystals of the complex with NADH–Me_2SO (Eklund et al., 1981).

Data Collection and Data Processing. X-ray diffraction measurements for all complexes were collected on a Stoe four-circle diffractometer using a step-scan procedure (Söderberg et al., 1974). The measured data were processed as described earlier (Eklund et al., 1976, 1981). Some data from these calculations are summarized in Table I.

Electron Density Maps and Interpretation. Crystallographic analysis of a number of alcohol dehydrogenase derivatives isomorphous to the apoenzyme has previously been made from difference Fourier calculations with the orthorhombic apoenzyme structure [see Brändén & Eklund (1980) for references] by using isomorphous phase angles. This structure has subsequently been refined (T. A. Jones, unpublished results), giving a more reliable structure determination (present R factor at 2.4-Å resolution is 21%). Using this refined model, we can now determine the structures of apoenzyme complexes to a higher degree of accuracy.

For triclinic ternary complexes except with NADH–Me_2SO, the situation has been different, and so far only a preliminary report at low resolution for the trifluoroethanol and bromobenzyl alcohol complexes (Plapp et al., 1978) has been given. Many ternary complexes, for example, enzyme–NAD^+–pyrazole, are very similar to the NADH–Me_2SO complex, and the important differences are details at the active site. The refinement of the enzyme–NADH–Me_2SO complex has now reached a satisfactory stage with an R factor of 26% at 2.9 Å (H. Eklund and T. A. Jones, unpublished results). Isomorphous complexes can now be solved by using the protein part of the refined complex as a starting model. The coenzyme and third ligand can easily be positioned from difference maps. Any change in conformation of the protein can also be detected.

During the course of the work, difference electron density maps were calculated to qualitatively establish the positions of the heterocyclic rings, coenzyme, zinc atoms, and zinc ligands. These interpretations guided us to what kind of difference maps to calculate for the final interpretation. Maps with coefficients $F_{obsd} - F_{nat}$, $F_{obsd} - F_{calcd}$, and $2F_{obsd} - F_{calcd}$ were computed for the binary complexes, where F_{obsd} is the observed F values for the derivative, F_{nat} the observed F values for native enzyme, and F_{calcd} the structure factors calculated form the refined model of the apoenzyme. Phases calculated from this model were used (a list of maps used is available; see paragraph at end of paper regarding supplementary material).

For the ternary complexes, difference Fourier maps were first calculated with coefficients $F_{obsd} - F_{calcd}$. The structure factors were calculated from the refined model of the ternary complex of alcohol dehydrogenase with NADH–Me_2SO but without the contribution of the inhibitor Me_2SO and the side chains of the following residues of each subunit: Ser-48, Leu-57, Phe-93, Leu-116, Leu-141, Val-294, Met-306, Leu-309, and Ile-318. The positions of the side chains of these residues, which line the substrate pocket, were examined in the difference maps and in some cases adjusted. The positions of the coenzyme molecules were examined in similar maps where the structure factors were calculated with contributions from the protein and Zn atoms, but not from coenzymes and Me_2SO molecules. The final positionings of inhibitor molecules were done from maps with coefficents $F_{obsd} - F_{calcd}$ and $2F_{obsd} - F_{calcd}$ with phases and structure factors calculated from the protein, coenzyme molecules, and Zn atoms positioned from earlier maps.

All maps were examined in a Vector General 3404 interactive graphics display by using Alwyn Jones' RING and FRODO programs (Jones, 1978, 1982). Dictionary values for the inhibitors were made by using distances and angles from X-ray and neutron studies (Ehrlich, 1960; Reimann et al., 1967; Krebs Larsen et al., 1970). Stereo diagrams were plotted on a Hewlett-Packard plotter by using computer programs written by T. A. Jones.

Model Building Experiments. The interactive graphics display was used for model building of substituted pyrazoles and of Zn–H_2O complexes. Substituted pyrazoles were constructed from the 4-iodopyrazole complex. Chemical groups were introduced with the FRODO program (Jones, 1982) and were attached to the pyrazole ring so that proper stereochemistry was obtained. The inital extended conformation of the alkyl chain was then changed when necessary by torsions around its bonds to avoid too close contacts. The pyrazole ring was not moved at all during the model building. No modification of the protein conformation was made with the exception of the side chain of Leu-116 for which different positions were investigated by changing its torsion angles.

Results

Binary Complexes. The binding of imidazole was earlier deduced from a difference Fourier map by using isomorphous replacement phases and differences between observed structure factors from the binary imidazole–enzyme complex and the

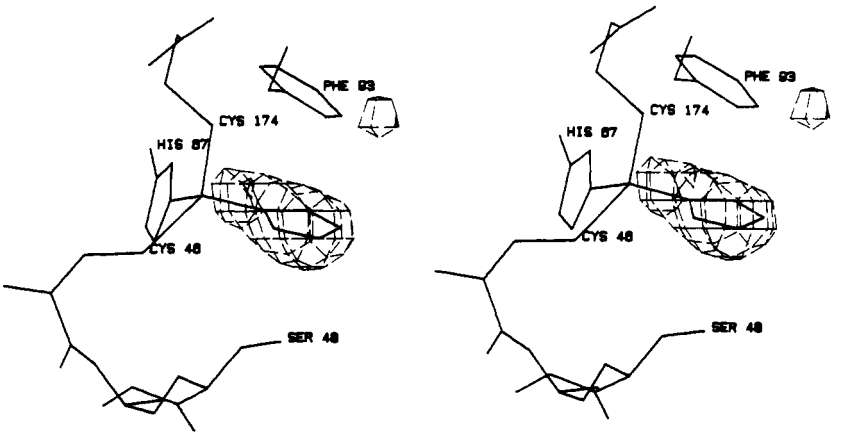

FIGURE 1: Stereo diagram of the active site of alcohol dehydrogenase with imidazole bound to the active-site zinc atom. The difference electron density is between the observed structure factors of the imidazole complex and the structure factors calculated from the native structure.

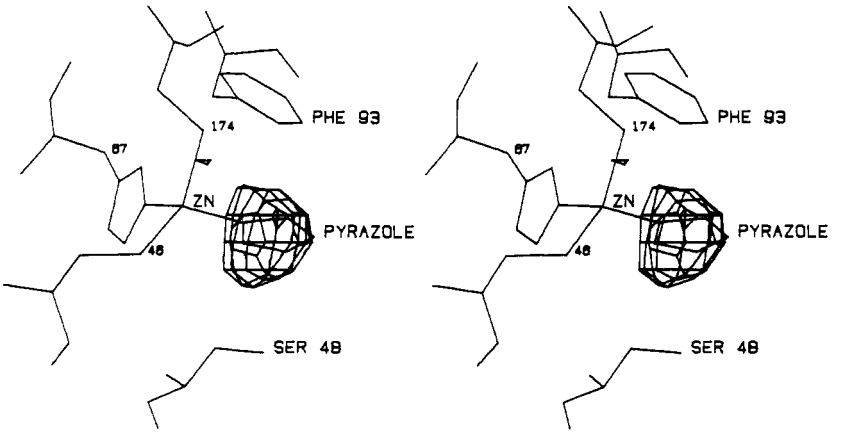

FIGURE 2: Pyrazole molecule positioned in difference electron density ($F_{obsd} - F_{calcd}$).

native protein (Boiwe & Brändén, 1977). As a complement to the present experimental studies, we reexamined the binding of imidazole using the refined protein structure and the interactive graphics display facilities. The binding we observe is similar to the one previously described except for a difference in the orientation of the plane of the imidazole ring. Both interpretations position the ring within the present electron density. Imidazole binds directly to the active metal, completing a roughly tetrahedral coordination (Table II) of the zinc atom (Figure 1). The water molecule that is bound to the active-site zinc atom in the native structure as well as an MPD molecule further down the substrate cleft is displaced for obvious steric reasons.

A narrow slit between the side chains of phenylalanine-93 and the side chain of serine-48 forms the entrance to the inner parts of the active site close to the zinc atom. The size of the imidazole molecule fits this slit, and the ring binds with its flat surface at van der Waals contact to the surface of the phenylalanine ring of residue 93 (Figure 1). The zinc position in the imidazole complex is slightly shifted toward the imidazole compared to its position in the native enzyme as deduced from the $2F_{obsd} - F_{calcd}$ map. The side chain of Ser-48 is hydrogen bonded to the zinc-bound water in the native enzyme. When water is replaced by imidazole, the side chain turns away from the zinc atom. This new position is obtained by a 20° torsion around the Cα–Cβ bond. Distances from atoms of the imidazole to the zinc and neighboring protein atoms are listed in Table III.

The difference electron density peak for the pyrazole molecule in the binary LADH–pyrazole complex has a lower level than the corresponding imidazole difference peak due to lower concentration of the inhibitor (Table I). The highest

Table II: Bond Angles Subtended at the Active-Site Zinc Atom in Imidazole and Pyrazole Complexes of LADH[a]

	binary complexes		ternary complexes, pyrazole/ 4-iodo-pyrazole
	H_2O in native enzyme[b]	imidazole/ pyrazole	
S46-Zn-N67	113		109
S46-Zn-S174	127		129
N67-Zn-S174	105		108
S46-Zn-ligand	108	120	107
N67-Zn-ligand	101	94	91
S174-Zn-ligand	100	94	98

[a] Average values are given in degrees. [b] T. A. Jones, unpublished results.

peak in the difference density map ($F_{der} - F_{nat}$) has been assigned to the pyrazole molecule. This peak is in a similar position as the corresponding peak for imidazole. The binding mode of pyrazole is essentially the same as that of imidazole with direct binding to the active-site zinc atom. The orientation of the plane of bound pyrazole is more difficult to establish than for imidazole due to the lower occupancy of pyrazole binding as well as the lower resolution of the pyrazole maps (Figure 2). By combining the observations from the different types of maps available, we built the pyrazole molecule in its most probable conformation. The resulting position for the pyrazole molecule differs only slightly from the observed imidazole position, and this difference is within the limits of error of the investigation. The pyrazole (like imidazole) ring plane is roughly coplanar with the ring plane of Phe-93 and almost perpendicular to the plane of His-67,

Table III: Interactions between LADH, NAD^+, and Bound Pyrazole and Imidazole[a]

pyrazole ternary complex		4-iodopyrazole ternary complex		pyrazole binary complex		imidazole binary complex	
N2	Cys-46 Sγ Ser-48 Cβ, Oγ His-67 Cδ2, Nε2 Cys-174 Sγ Zn (act.) (2.1 Å) NAD, C4N, C5N	N2	Cys-46 Sγ Ser-48 Cβ, Oγ His-67 Cδ2, Cε1, Nε2 Cys-174 Sγ Zn (act.) (2.1 Å) NAD, C4N, C5N	N2	Ser-48 Oγ His-67 Cδ2, Cε1, Nε2 Cys-174 Sγ Zn (act.) (2.1 Å)	N1	Ser-48 Oγ His-67 Nε2 Cys-174 Sγ Zn (act.) (2.1 Å)
C3	Ser-48 Cβ, Oγ His-67 Cδ2, Cε1, Nε2 Zn (act.)	C3	Ser-48 Cβ, Oγ His-67 Cε1, Nε2 Zn (act.)	C3	Ser-48 Cβ, Oγ His-67 Cδ2, Cε1, Nε2 Zn (act.)	C5	Ser-48 Cβ, Oγ His-67 Cε1, Nε2 Zn (act.)
C4	Ser-48 Cβ, Oγ	C4	Ser-48 Cβ, Oγ	C4	Ser-48 Cβ, Oγ	C4	Ser-48 Cβ, Oγ Phe-93 Cε2
C5	Ser-48 Oγ NAD C2N, C3N, C4N, C5N, C7N	C5	Ser-48 Oγ NAD C2N, C3N, C4N, C5N, C7N, O1N	C5	Ser-48 Oγ	N3	Ser-48 Oγ
N1	Ser-48 Oγ Cys-174 Sγ Zn (act.) NAD C2N, C3N, C4N (2.0 Å), C5N, C6N, C7N, O1N	N1	Ser-48 Oγ Cys-174 Sγ Zn (act.) NAD N1N, C2N, C3N, C4N (2.0 Å), C5N, C6N, C7N, O1N	N1	Ser-48 Oγ Cys-174 Sγ Zn (act.)	C2	Ser-48 Oγ Cys-174 Sγ Zn (act.)
		I	Ser-48 Cβ, Oγ Leu-57 Cβ, Cδ2 Phe-93 Cδ2, Cε2 Leu-116 Cβ, Cγ, Cδ2 Leu-141 Cδ1, Cδ2 Val-294 Cγ2				

[a] Atoms closer than 3.8 Å from bound imidazole and pyrazole molecules are listed in the table. Phenylalanine-93 is close to many atoms in the bound ligands, but the distances are slightly longer than 3.8 Å and are not included in the table. Atoms closer than 5 Å to the iodine atom of 4-iodopyrazole are also listed.

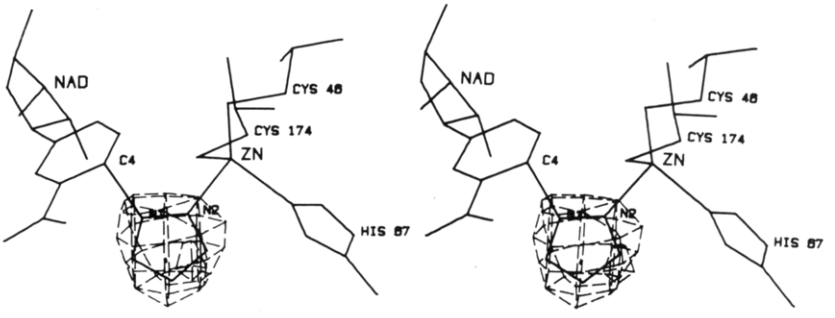

FIGURE 3: Pyrazole positioned in a $F_{obsd} - F_{calcd}$ map. A bond is drawn between the C4 position of the nicotinamide ring and N1 of the pyrazole ring.

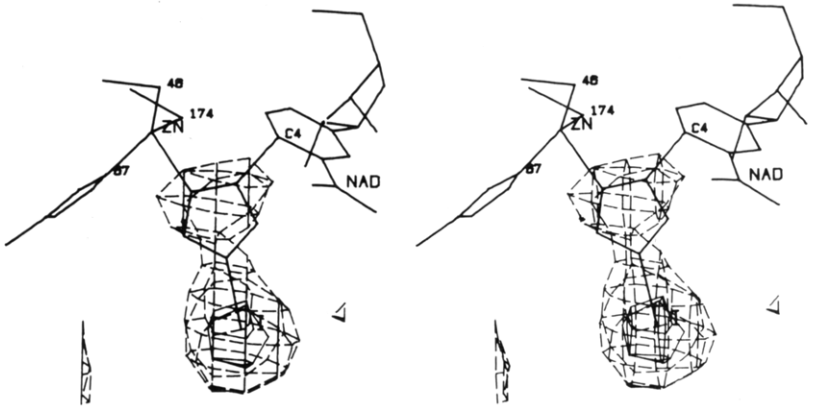

FIGURE 4: Molecule of 4-iodopyrazole positioned in its difference density ($F_{obsd} - F_{calcd}$).

a ligand to the active-site zinc atom.

Ternary Complexes. The electron density maps were computed independently for each subunit in the ternary complexes. In each case, they showed very similar features, and no significant difference between the active-site region in the two subunits could be detected. Electron density maps of the enzyme–NAD^+–pyrazole complex clearly show a flat density between the active-site zinc atom and the nicotinamide ring of the coenzyme. A pyrazole molecule placed in this density is shown in Figure 3.

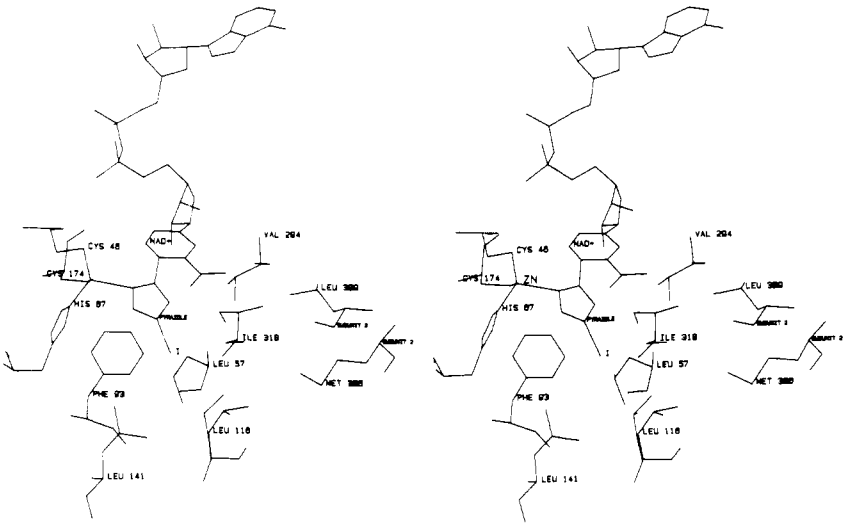

FIGURE 5: Stereo diagram of 4-iodopyrazole bound at the active site in alcohol dehydrogenase. The diagram shows the binding of 4-iodopyrazole in relation to the hydrophobic substrate cleft. The side chain of Leu-116 is shown in its position both in the enzyme NAD^+–pyrazole complex and in the enzyme NAD^+–4-iodopyrazole complex. The side chain has moved away from the ligand in the latter complex due to its bulky substituent.

The electron density maps of 4-iodopyrazole have the same flat density between the active-site zinc atom and the nicotinamide ring as those of the unsubstituted pyrazole. Connected to this flat density is a very strong spherical electron density peak corresponding to the iodine atom (Figure 4). Positioning of the 4-iodopyrazole in its density is straightforward, since the strong iodine peak allows an accurate positioning of the pyrazole ring.

When the electron density maps of these ternary complexes were interpreted, the iodopyrazole molecule was first positioned in density with its iodine atom in the middle of the strong spherical density. The N2 nitrogen atom then automatically becomes positioned within binding distance of the active-site zinc atom when the pyrazole ring is placed in its flat density. The other nitrogen atom is then 2.0 Å from the C4 carbon of the nicotinamide ring. The direction of this bond is roughly perpendicular to the nicotinamide ring. The model building of the pyrazole ring in the ternary complex enzyme–NAD^+–pyrazole used this observed position of the pyrazole ring in the iodopyrazole molecule as the starting position. The pyrazole ring then had to be changed slightly to fit the density in the best way (Figure 3). The binding is nevertheless very similar, and the positions of the two nitrogen atoms with respect to the zinc atom and the C4 atom of the nicotinamide ring are very similar. The pyrazole ring in the iodopyrazole complex has a slightly different tilt than in the pyrazole complex. The C4 atom of the iodopyrazole differs by a few tenths of an angstrom from its position in the unsubstituted pyrazole due to interactions of the iodine atom with the side chain of Leu-57. The stereo diagram of the 4-iodopyrazole molecule bound in its ternary enzyme–NAD^+ complex is shown in Figure 5. The nearest neighbors of the atoms in the pyrazole and 4-iodopyrazole molecules are listed in Table III.

The binding position of bound pyrazole in these ternary complexes is quite similar to that of imidazole and pyrazole in the binary complexes. The ring is bound between the side chains of Ser-48 and Phe-93, roughly parallel to the phenyl ring of residue 93. The plane of the ring of His-67 and the nicotinamide ring are also roughly perpendicular to the ring plane of pyrazole. The pyrazole ring is thus enclosed within the rings of residues Phe-93 and His-67, the nicotinamide ring of the coenzyme, and the side chain of Ser-48 in the narrow active site. The side-chain oxygen atom of Ser-48 is pointing away from the zinc atom as observed in the binary complexes. This residue makes a hydrogen bond to O2′ of the nicotinamide ribose as observed in all refined ternary complex structures (H. Eklund, J.-P. Samama, C.-I. Brändén, and T. A. Jones, unpublished results).

Coenzyme Binding. The conformations of the NAD molecules were examined in difference Fourier maps calculated without any contribution from coenzyme atoms. No significant deviation could be detected in the ADP-ribose part from the conformation observed for NADH in the enzyme–NADH–Me_2SO complex (Eklund et al., 1981). However, a slight tilt of the nicotinamide ring was required in order to fit the density in the best way. The interactions of the coenzyme with the protein were examined in maps with coefficients $2F_{obsd} - F_{calcd}$. All interactions were essentially the same as observed in other ternary complexes which are described elsewhere (H. Eklund, J.-P. Samama, C.-I. Brändén, and T. A. Jones, unpublished results).

Active-Site Residues. Maps with coefficients $F_{obsd} - F_{calcd}$ where the active-site residues have been removed from the calculations are very useful for detecting differences in the positions of the omitted residues. No changes from the NADH–Me_2SO complex in the position of the active-site zinc atom of each subunit or its ligands are observed in difference electron density maps with these parts subtracted. In addition, no changes are observed for the residues of the substrate cleft in the NAD^+–pyrazole complex compared to the NADH–Me_2SO complex. However, for the NAD^+–4-iodopyrazole complex, the conformation of Leu-116 is different. The side chain of this residue turns around its $C\alpha$–$C\beta$ and $C\beta$–$C\gamma$ bonds, thereby widening the substrate cleft to accommodate the bulky iodine atom. This is shown in Figure 5. Similar changes have been observed for other large ligands like *p*-bromobenzyl alcohol (Eklund et al., 1982) and (dimethylamino)cinnamaldehyde (Cedergren-Zeppezauer et al., 1982).

Substitutions on the Pyrazole Molecule. In order to be able to relate the binding properties of 4-substituted pyrazole derivatives to the topography of the substrate cleft, we did model-building experiments with a linear 12-carbon alkyl chain attached to the pyrazole ring in the 4 position. We started with a staggered extended chain, and only small torsions had to be applied to the bonds between carbons 4 and 5 (10°) and

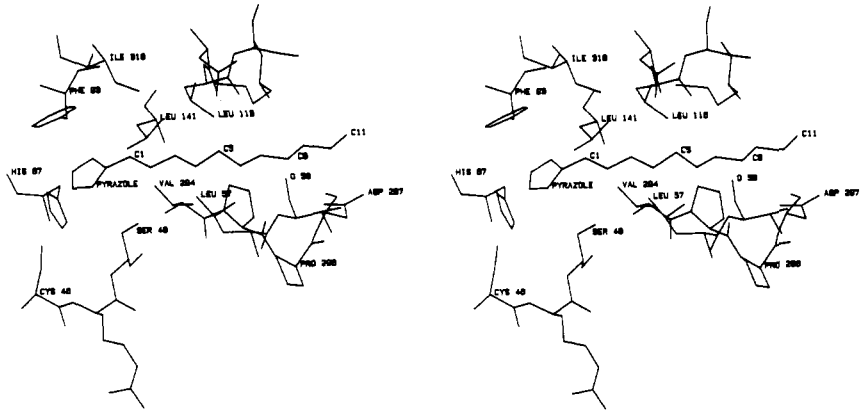

FIGURE 6: Hydrophobic channel in alcohol dehydrogenase surrounding the 4-alkylpyrazole chain which was positioned by model building. The view is perpendicular to the alkyl chain.

carbons 6 and 7 (20°) to fit the alkyl chain to the long hydrophobic substrate channel which extends from the active site to the solution. This channel is rather narrow close to the active-site zinc atom between His-67, Phe-93, and Ser-48, which limit the space where the pyrazole ring binds. The channel is then somewhat wider around carbon atoms 1–3 of the alkyl chain before it again narrows between Leu-57, Leu-116, and Val-294. The side chain of Leu-116 has been observed to change its conformation according to the size of the bound ligand. This side chain has to be turned slightly from its position in 4-iodopyrazole to make room for the fifth carbon atom of the alkyl chain. After this narrow passage, the channel widens toward the solution from carbon atom 6 and onward, and at the same time the character of the channel becomes more polar. A number of different positions of the alkyl side chain can easily be fitted to the enzyme model in this region. A stereo diagram of one of these conformations based on the most extended alkyl chain is given in Figure 6. The protein atoms closest to the alkyl chain are listed in Table IV.

Table IV: Environment of the Carbon Atoms in a Linear Alkyl Chain Attached at the 4 Position to a Bound Pyrazole Molecule[a]

chain position	interacting amino acid	interacting atoms
C1	Ser-48	Oγ
C2	Ser-48	Oγ
	Leu-57	Cδ2
	Val-294	Cγ2
C3	Leu-57	Cδ2
	Leu-116	Cγ, Cδ2
C4	Leu-57	Cδ2
	Leu-116	Cδ2
	Val-294	Cγ1, Cγ2
C5	Leu-57	Cδ2
	Leu-116	Cγ, Cδ1, Cδ2
	Val-294	Cγ1
C6	Leu-57	Cα, Cδ2
	Leu-116	Cδ2
C7	Leu-57	Cδ1
	Val-58	N
C8	Val-58	N
	Asp-297	Oδ1
C9	Val-58	O
C10	Asp-297	Cγ, Oδ1, Oδ2
C11	solvent region starts	

[a] The alkyl chain is positioned by model building. Protein atoms closer than 4 Å are listed.

Discussion

The refinement of the two forms of alcohol dehydrogenase has considerably reduced the errors in the model of the protein structure. The average random errors in the coordinates are generally as low as a few tenths of an angstrom unit over the whole protein but may be larger locally. The availability of the interactive graphic display system makes positioning of model atom more accurate than the earlier use of the mirror arrangements (Richards, 1968). The electron density is easier to interpret since it is possible to view from different directions and the interaction with neighboring atoms can be followed during the model building. Protein parts can usually be built with more precision than bound ligands because the sequential protein structure gives more accurate densities with obvious branch points for side chains and carbonyl oxygen atoms.

The restrictions in model building are less severe for ligands bound to the enzyme. The interpretation of the 4-iodopyrazole map is, however, unusually straightforward, since the iodine atom can be positioned with high accuracy. This introduces severe restrictions on positioning of the attached pyrazole ring within its electron density.

Binding to the Active-Site Zinc Atom. Imidazole has earlier been shown by X-ray diffraction studies to bind directly to the active-site zinc atom in the binary complex with liver alcohol dehydrogenase (Boiwe & Brändén, 1977). This conclusion is confirmed by the present more accurate study. Pyrazole is also found to bind directly to zinc in both the binary complex and the ternary complexes. Direct binding to zinc of imidazole and pyrazole is also in agreement with solution studies using a number of different methods (Theorell & McKinley-McKee, 1961; Theorell & Yonetani, 1963; Theorell et al., 1969; Shore & Gilleland, 1970; Reynolds & McKinley-McKee, 1972; Andersson, P., et al., 1981; Andersson, I., et al., 1981; Makinen & Yim, 1981). Contradictory conclusions have, however, been reported from NMR experiments with metal-sustituted enzymes. These observations were interpreted in terms of indirect binding via a water molecule to the active-site metal atom. This has been reported for both imidazole (Young & Mildvan, 1977) and pyrazole (Bobsein & Meyers, 1980) by using Co and Cd NMR studies, respectively.

The conclusions for the Co enzyme were based on small changes observed at 100 MHz attributed to paramagnetic effects. These changes have been shown to be within the variations of the diamagnetic contribution upon metal ion substitution (Andersson, I., et al., 1981). Thus distance calculations based on these variations must be highly questionable. From chemical shift studies in solution of ^{113}Cd-substituted enzyme Bobsein & Meyers (1980, 1981) have concluded that imidazole binds directly to cadmium and that pyrazole binds indirectly.

We have done model-building experiments, placing a water molecule between the zinc atom and the imidazole or pyrazole

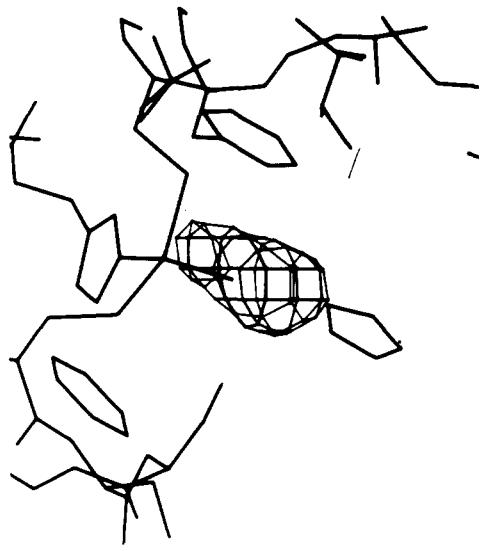

FIGURE 7: Photograph of the display picture after model building of imidazole bound via a water molecule to the zinc. The imidazole was placed at hydrogen bond distance to the zinc-bound water. The difference electron density map ($F_{obsd} - F_{calcd}$) is superimposed. Figure 1 shows direct binding of imidazole to the active-site zinc atom.

ring. In these experiments we used the native coordinate set as the starting point. The zinc atom in the native enzyme has a water molecule bound to zinc. The imidazole and the pyrazole molecules were placed at hydrogen bond distance to the water. Figure 7 shows that it is then impossible to fit the ligand into its experimentally determined density. It is obvious that his mode of binding is inconsistent with the crystallographic results. Difference density maps of the type $F_{der} - F_{nat}$ give strong difference densities in the vicinity of the zinc atom that clearly show that there is a ligand different from a water molecule bound to the zinc atom in the binary complexes. Other crystallograhic studies on ternary complexes also show direct binding of ligands to the Zn atom. For example direct binding has been observed for Me_2SO (Eklund et al., 1981), bromobenzyl alcohol (Eklund et al., 1982), and (dimethylamino)cinnamaldehyde (Cedergren-Zeppezauer et al., 1982) which have all been studied in ternary complexes to 2.9-Å resolution.

The distance of 7.1 Å between the side chains of Phe-93 and Ser-48 allows room for a flat ring like imidazole or pyrazole. In this position the heterocyclic compound has van der Waals contacts with both residues and a direct coordination to Zn. We also found that the plane of the ligand and the ring of Phe-93 were different by 20–30°. Pyrazole is furthermore restricted in its position by His-67 on one side and by nicotinamide on the other. The heterocyclic ring can, however, rotate around the bond between the ligand and the Zn atom by a maximum amount of ±20° from its observed position.

Binding of Pyrazole to the Coenzyme in Ternary Complexes. When the pyrazole ring in the two ternary complexes LADH–NAD^+–pyrazole and LADH–NAD^+–4-iodopyrazole is placed in density with the N2 nitrogen atom bound to the zinc atom, then the second nitrogen atom comes close to the nicotinamide ring. The distance between the pyridinium C4 and pyrazole N1 atoms is 2 Å. This is 0.5 Å longer than a typical covalent bond. The C4–N1 bond is approximately normal to the plane of the nicotinamide ring. Deviations from typical covalent bond lengths have earlier been reported both in organic compounds (Bürgi et al., 1973) and in enzyme complexes (James et al., 1980) and may turn out to be a common phenomenon in intermediate complexes in enzyme catalysis. The mode of binding is similar in both subunits.

Kinetic experiments (Andersson, P., et al., 1981) have shown that the N1 pyrazole hydrogen undergoes a drastic pK_a shift when the inhibitor is coordinated to the Zn atom. Pyrazole has been proposed to be covalently bound to the pyridinium ring in NAD^+ (Theorell & Yonetani, 1963) under strong basic conditions in the absence of enzyme. This covalent interaction has been suggested mainly because it explains the UV absorption band at 290 nm. Dihydropyridine addition compounds are absorbing in this region (Kaplan, 1960). Similar absorption bands have been found in nonenzymatic NAD^+ complexes with hydroxylamine (Kaplan & Ciotti, 1954), cyanide ions (Meyerhof et al., 1938), and other small nucleophilic molecules (van Eys et al., 1958). When these addition complexes are formed in the presence of liver alcohol dehydrogenase, there is a 10–15-nm blue shift in their UV absorption spectra (van Eys et al., 1958). This could be induced by the water-free partly hydrophobic environment of the active site and by a coordination to the Zn atom, similar to that seen here with pyrazole.

Much effort has been devoted to studies of the bonds in pyridine addition compounds (Wallenfels & Schüly, 1959) in the hope of getting further information on the reduction step in the enzyme mechanism. The binding mode observed here might strengthen the idea (Theorell & Yonetani, 1963) that alcohol dehydrogenase, pyrazole, and NAD^+ together form a transition-state similar inhibitor complex.

Differences between Pyrazole and Imidazole. The binary complexes of pyrazole and imidazole with liver alcohol dehydrogenase are very similar. This is a consequence of the fact that the inner part of the active site is narrow and does not allow much flexibility in the binding of these inhibitors. However, the ability to form ternary complexes with coenzyme and enzyme is very different for the two inhibitors. While pyrazole only forms a strong ternary complex with NAD^+ and liver alcohol dehydrogenase (Theorell et al., 1969; McFarland & Bernhard, 1972), imidazole forms weak ternary complexes with either form of the coenzyme. This can be due to differences in the acid–base properties of pyrazole and imidazole. The pK_a for the acidic form of imidazole is 7 while it is 2.5 for pyrazole. This difference may also influence the next pK value for the two rings such that the pyrazole molecule may more easily form a negative ion than imidazole when bound to the enzyme. This may be a necessary part of strong complex formation in order to balance the positive charge of the nicotinamide ring in NAD^+ as suggested by Theorell & Yonetani (1963).

Furthermore, there is a difference in the position of the second nitrogen atom within the ring. In the model deduced from the electron density maps, the N1 atom of pyrazole comes close to C4 of the nicotinamide ring. Under the assumption that it would be an imidazole ring, the free nitrogen would then be pointing toward the C3 atom of the nicotinamide. To make a bond between this nitrogen and the C4 position would require a severe rearrangement in the positioning of NAD^+ and/or imidazole.

Substitution Effects. The large increase in inhibitory power of pyrazole when there are substitutions at the 4 position is a consequence of the position of the pyrazole ring in the substrate cleft (Figures 5 and 6). Hydrophobic substituents in this position increase the number of interactions with the hydrophobic residues of the substrate cleft and thereby also increase the stability of the enzyme–NAD^+–inhibitor complex. On the other hand substitutions at the 5 position sterically interfere with the coenzyme (Figure 8) and thus weaken the binding (Theorell et al., 1969; Fries et al., 1979). Substitutions

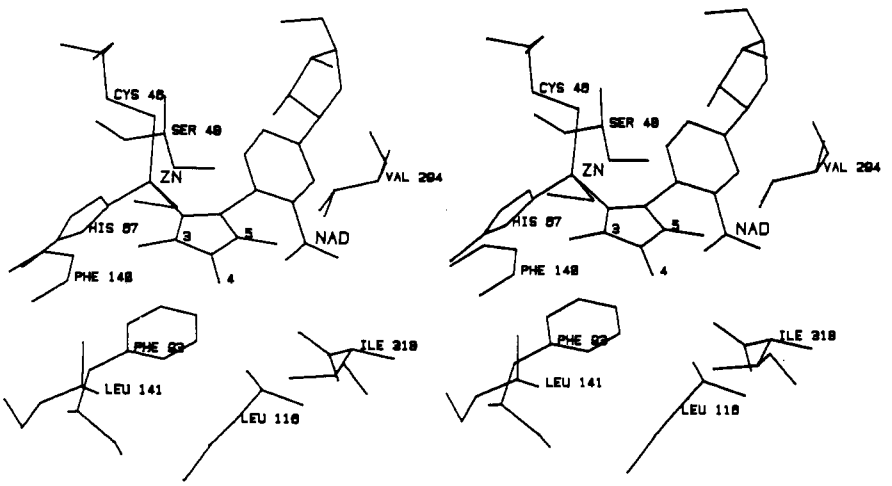

FIGURE 8: Model of 3,4,5-trimethylpyrazole placed at the active site of the enzyme. The model of the derivative is constructed from a 4-iodopyrazole molecule as bound to the enzyme in the ternary complex.

Table V: Inhibitory Power of Some 4-Substituted Pyrazoles Chosen from the Large Number of Substituted Derivatives Described in the Literature (Tolf, 1981)

R	K_I (μM)	reference
H	0.22	Theorell et al. (1969)
CH_3	0.13[c]	Dahlbom et al. (1974)
CH_2CH_3	0.007	Tolf et al. (1979)
$(CH_2)_2CH_3$	0.004	
$(CH_2)_3CH_3$	0.0018[b]	
$(CH_2)_4CH_3$	0.0008[b]	
$(CH_2)_5CH_3$	0.0005[b]	
$(CH_2)_6CH_3$	0.0003[b]	
$(CH_2)_7CH_3$	<0.0003[a]	
$(CH_2)_{10}CH_3$	<0.0003[a]	
$(CH_2)_{13}CH_3$	<0.0003[a]	
$(CH_2)_3N^+(CH_3)_3$	800	Tolf (1981)
$(CH_2)_4N^+(CH_3)_3$	50	
$(CH_2)_7N^+(CH_3)_3$	0.0115	
$(CH_2)_3COOH$	15	Tolf (1981)
$(CH_2)_4COOH$	2	

[a] Too low to be measured. [b] Corrected for the amount of inhibitor bound by the enzyme. [c] K_I = 0.08 μM in Theorell et al (1969).

at the 3 position make too close contacts with His-67 and Ser-48. Substitutions at both the 3 and 5 positions make the pyrazole derivative too bulky to have simultaneous binding of the nicotinamide ring and inhibitor in the active site. These results are obvious and were essentially suggested from model-building studies (Brändén, 1977) based on knowledge of the active site of the apoenzyme and the proposed mode of binding by Theorell & Yonetani (1963).

Inhibitory constants for a number of linear 4-alkyl derivatives of pyrazole are given in Table V. Examination of this table shows that linear alkyl 4 substituents give stronger affinity as the size of the chain is increased. Positively or negatively charged groups on the other hand decrease the affinity unless they are remote from the pyrazole ring. In these latter cases, they reach polar residues at the bottom of the substrate binding site, close to the outer solution (Table IV). Branched and bulky substituents sterically interfere with protein residues along the rather narrow hydrophobic channel.

There is a large difference between yeast and liver alcohol dehydrogenase (Reynier, 1969) on the effect of substitutions made at the 4 position of the pyrazole ring. Such substitutions drastically decrease the inhibitory power of the derivative with yeast alcohol dehydrogenase. This can be correlated with differences in the amino acid sequence in the active site (Jörnvall et al., 1978) which decreases the space available for substrate or inhibitor binding.

Acknowledgments

We thank Dr. Å. Åkeson and G. Lundquist for gifts of purified enzyme, Dr. M. Zeppezauer for the gift of 4-iodopyrazole, T. Boiwe for use of his X-ray diffraction data of imidazole binary complex, and T. A. Jones for making the refined apoenzyme coordinates available.

Supplementary Material Available

A table listing the different maps used in this investigation and a table with coordinates for imidazole, pyrazole, and 4-iodopyrazole in the different complexes and the coordinates of the active-site zinc atom, its ligands, and the C4 atom of NAD (5 pages). Ordering information is given on any current masthead page.

References

Andersson, I., Maret, W., Zeppezauer, M., Brown, R. D., III, & Koening, S. H. (1981) *Biochemistry 20*, 3424–3432.

Andersson, L., Jörnvall, H., Åkeson, Å., & Mosbach, K. (1974) *Biochim. Biophys. Acta 364*, 1–8.

Andersson, P., Kvassman, J., Lindström, A., Oldén, B., & Pettersson, G. (1981) *Eur. J. Biochem. 113*, 425–433.

Blomstrand, R., & Theorell, H. (1970) *Life Sci. 9*, 631–640.

Bobsein, R. B., & Myers, J. R. (1980) *J. Am. Chem. Soc. 102*, 2454–2455.

Bobsein, R. B., & Myers, J. R. (1981) *J. Biol. Chem. 256*, 5313–5316.

Boiwe, T., & Brändén, C.-I. (1977) *Eur. J. Biochem. 77*, 173–179.

Bosron, W. F., Li, T.-K., Dafeldecker, W. P., & Vallee, B. L. (1979) *Biochemistry 18*, 1101–1105.

Brand, L., Gohlke, R. J., & Sethu Rao, D. (1967) *Biochemistry 6*, 3510–3518.

Brändén, C.-I. (1965) *Arch. Biochem. Biophys. 112*, 215–217.

Brändén, C.-I. (1977) in *Pyridine Nucleotide-dependent Dehydrogenases* (Sund, H., Ed.) pp 325–338, de Gruyter, Berlin and New York.

Brändén, C.-I., & Eklund, H. (1980) in *Dehydrogenases Requiring Nicotinamide Coenzymes* (Jeffrey, J., Ed.) pp 41–84, Birkhäuser Verlag, Basel.

Brändén, C.-I., Larsson, L.-M., Lindqvist, I., Theorell, H., & Yonetani, T. (1965) *Arch. Biochem. Biophys. 109*, 195.

Bürgi, B. H., Dunitz, J. D., & Shefter, E. (1973) *J. Am. Chem. Soc. 95*, 5065–5067.

Cedergren-Zeppezauer, E., Samama, J.-P., & Eklund, H. (1982) *Biochemistry* (in press).

Dahlbom, R., Tolf, B. R., Åkeson, Å., Lundquist, G., & Theorell, H. (1974) *Biochem. Biophys. Res. Commun. 57*, 549–553.

Deis, H. L., & Lester, D. (1979) *Biochem. Pharmacol. Ethanol 1*, 303–323.

De Traglia, M. C., Schmidt, J., Dunn, M. F., & McFarland, J. T. (1977) *J. Biol. Chem. 252*, 3493–3500.

Ehrlich, H. W. W. (1960) *Acta Crystallogr. 13*, 946–952.

Eklund, H., Nordström, B., Zeppezauer, E., Söderlund, G., Ohlsson, I., Boiwe, T., Söderberg, B.-O., Tapia, O., & Brändén, C.-I. (1976) *J. Mol. Biol. 102*, 27–59.

Eklund, H., Samama, J.-P., Wallén, L., Brändén, C.-I., Åkeson, Å., & Jones, T. A. (1981) *J. Mol. Biol. 146*, 561–587.

Eklund, H., Plapp, B. V., Samama, J.-P., & Brändén, C.-I. (1982) *J. Biol. Chem.* (in press).

Fries, R. W., Bohlken, D. P., & Plapp, B. V. (1979) *J. Med. Chem. 22*, 356–359.

Jacobs, W. J., McFarland, T. J., Wainer, I., Jeanmaier, D., Ham, D., Hamm, K., Wnuk, M., & Lamm, M. (1974) *Biochemistry 13*, 60–64.

James, M. N. G., Sielecki, A. R., Brayer, G. D., Delbaere, L. T. J., & Bauer, C.-A. (1980) *J. Mol. Biol. 144*, 43–88.

Jones, T. A. (1978) *J. Appl. Crystallogr. 11*, 268–272.

Jones, T. A. (1982) *Computational Crystallography* (Sayre, D., Ed.) pp 303–317, Oxford University Press, Oxford.

Jörnvall, H., Eklund, H., & Brändén, C.-I. (1978) *J. Biol. Chem. 253*, 8414–8419.

Kaplan, N. O. (1960) *Enzymes, 2nd Ed. 3*, 105–169.

Kaplan, N. O., & Ciotti, M. (1954) *J. Biol. Chem. 211*, 431–445.

Krebs Larsen, F., Lehmann, M. S., Søtofte, I., & Rasmussen, S. E. (1970) *Acta Chem. Scand. 24*, 3248–3258.

Lange, G. L., & Vallee, B. L. (1976) *Biochemistry 15*, 4681–4686.

Lester, D., Keokosky, W. Z., & Felzenberg, F. (1968) *Q. J. Stud. Alcohol, Part A 29*, 449–454.

Li, T.-K. (1977) *Adv. Enzymol. Relat. Areas Mol. Biol. 45*, 427–483.

Li, T.-K., Bosron, W. F., Dafeldecker, W. P., Lange, L. G., & Vallee, B. L. (1977) *Proc. Natl. Acad. Sci. U.S.A. 74*, 4378–4381.

Lieber, C. S. (1977) in *Metabolic Aspects of Alcoholism*, pp 1–29, University Park Press, Baltimore, MD.

Luisi, P. L., Baici, A., Bonner, F. J., & Aboderin, A. A. (1975) *Biochemistry 14*, 362–368.

Makinen, M. W., & Yim, M. B. (1981) *Proc. Natl. Acad. Sci. U.S.A. 78*, 6221–6225.

Maret, W., Dietrich, H., Ruf, H.-H., & Zeppezauer, M. (1980) *J. Inorg. Biochem. 12*, 241–252.

McFarland, J. T., & Bernhard, S. A. (1972) *Biochemistry 11*, 1486–1492.

McFarland, J. T., Chen, J., Wnuk, M., De Traglia, M. C., Yuen Li, T., Petersen, R., Jacobs, J. W., Schmidt, J., Feinberg, B., & Watters, K. L. (1977) *J. Mol. Biol. 115*, 355–380.

Meyerhof, O., Ohlmeyer, P., & Möhle, W. (1938) *Biochem. Z. 297*, 113.

Plapp, B. V., Eklund, H., & Brändén, C.-I. (1978) *J. Mol. Biol. 122*, 23–32.

Reimann, C. W., Mighell, A. D., & Mauer, F. A. (1967) *Acta Crystallogr. 23*, 135–141.

Reynier, M. (1969) *Acta Chem. Scand. 23*, 1119–1129.

Reynolds, C. H., & McKinley-McKee, J. S. (1972) *FEBS Lett. 21*, 297–299.

Reynolds, C. H., & McKinley-McKee, J. S. (1975) *Arch. Biochem. Biophys. 168*, 145–162.

Richards, F. M. (1968) *J. Mol. Biol. 37*, 225–230.

Rydberg, U., Buijten, J., & Neri, A. (1972) *J. Pharm. Pharmacol. 24*, 651–652.

Shore, J. D., & Gilleland, M. J. (1970) *J. Biol. Chem. 245*, 3422–3425.

Söderberg, B.-O., Holmgren, A., & Brändén, C.-I. (1974) *J. Mol. Biol. 90*, 143–152.

Theorell, H., & McKinley-McKee, J. S. (1961) *Acta Chem. Scand. 15*, 1811–1833.

Theorell, H., & Yonetani, T. (1963) *Biochem. Z. 338* 537–553.

Theorell, H., & Tatemoto, K. (1971) *Arch. Biochem. Biophys. 142*, 69–82.

Theorell, H., Yonetani, T., & Sjöberg, B. (1969) *Acta Chem. Scand. 23*, 255–260.

Tolf, B.-R. (1981) Acta Universitatis Upsaliensis, Thesis at Faculty of Pharmacy.

Tolf, B.-R., Piechaczek, J., Dahlbom, R., Theorell, H., Åkeson, Å., & Lundquist, G. (1979) *Acta Chem. Scand., Ser. B 33*, 483–487.

van Eys, J., Stolzenbach, F. E., Sherwood, L., & Kaplan, O. N. (1958) *Biochim. Biophys. Acta 27*, 63–83.

Wallenfels, K., & Schüly, H. (1959) *Justus Liebigs Ann. Chim. 620*, 86–105.

Yonetani, T. (1963) *Biochem. Z. 338*, 300–316.

Young, J. M., & Mildvan, S. A. (1977) *Alcohol and Aldehyde Metabolizing Systems* (Thurman, R. G., Williamson, J. R., Drott, H. R., & Chance, B., Eds.) Vol II, pp 109–117, Academic Press, New York.

Zeppezauer, E., Söderberg, B.-O., Brändén, C.-I., Åkeson, Å., & Theorell, H. (1967) *Acta Chem. Scand. 21*, 1099–1101.